

RIS-Assisted Vehicular Network with Direct Transmission over Double-Generalized Gamma Fading Channels

Vinay Kumar Chapala, Arsalan Malik, and S. M. Zafaruddin

Department of Electrical and Electronics Engineering, BITS Pilani, Pilani Campus, Pilani-333031, Rajasthan, India
Email: {p20200110, f20190499, syed.zafaruddin}@pilani.bits-pilani.ac.in

Abstract—Reconfigurable intelligent surface (RIS) can provide stable connectivity for vehicular communications when direct transmission becomes significantly weaker with dynamic channel conditions between an access point and a moving vehicle. In this paper, we analyze the performance of a RIS-assisted vehicular network by coherently combining received signals reflected by RIS elements and direct transmissions from the source terminal over double generalized Gamma (dGG) fading channels. We present analytical expressions on the outage probability and average bit-error rate (BER) performance of the considered system by deriving exact density and distribution functions for the end-to-end signal-to-noise ratio (SNR) resulted from the finite sum of the direct link and product of channel coefficients each distributed according to the dGG. We also develop asymptotic analysis on the outage probability and average BER to derive diversity order for a better insight into the system performance at high SNR. We validate the derived analytical expressions through numerical and simulation results and demonstrate scaling of the system performance with RIS elements and a comparison to the conventional relaying techniques and direct transmissions considering various practically relevant scenarios.

Index Terms—Bit error rate, ergodic rate, Fox's H-function, outage probability, reconfigurable intelligent surface, vehicular networks.

I. INTRODUCTION

The upcoming 6G wireless system envisions to cater exceedingly higher requirements of network throughput, lower latency of transmission, and stable connectivity for autonomous vehicular communications [1]. However, dynamic channel conditions between an access point to a vehicle in motion may be a bottleneck for the desired quality of service. The use of reconfigurable intelligent surface (RIS) can be a promising technology to create a strong line-of-sight (LOS) transmissions by artificially controlling the characteristics of propagating signals for vehicular communications [1]–[3]. An RIS is a planar metasurface made up of a large number of inexpensive passive reflective elements that can be electronically programmed to customize the phase of the incoming electromagnetic wave for enhanced signal quality

and transmission coverage. As is for other wireless networks, it is desirable to analyze the applicability of RIS for vehicular communications as a proof of concept considering generalized deployment scenarios.

Recently, there has been an extensive study exploring the benefits of the RIS approach for variety of wireless communication networks such as radio-frequency (RF) [4]–[10], free-space optics (FSO) [11], [12], and terahertz (THz) [13], [14]. More specifically, the authors analyzed the performance of RIS-assisted RF systems over Rayleigh fading model in [4], Rician fading in [5], Nakagami-m channel model in [6], [7] and fluctuating two rays (FTR) fading model for RIS-assisted mmWave communications in [10]. The authors in [9] presented an exact performance analysis for RIS-assisted wireless transmissions over generalized Fox's H fading channels. In [12], a unified performance analysis for a FSO system was presented considering different atmospheric turbulence models and pointing errors. The authors in [13], [14] analyzed RIS-aided THz communications over different fading channel models combined with antenna misalignment and hardware impairments.

Considering the benefits for conventional wireless transmissions, the use of RIS has been recently proposed for connected autonomous vehicles and vehicular networks [15]–[20]. The authors in [15] used series expansion and the central limit theorem (CLT) to approximate the outage probability of RIS-assisted vehicular networks over Rayleigh and Rician fading channels. In [16], the authors analyzed the outage probability, average bit-error rate (BER), and ergodic capacity of a RIS-enabled mobile network with random user mobility. The authors [17] developed an iterative algorithm to optimize the RIS phase shifts for the data rate maximization of a RIS-assisted mmWave vehicular communication network. In [18], the authors studied the RIS-enabled vehicle-to-vehicle (V2V) communications using the Fox's H-function distribution. In [19], the placement of multiple RIS is optimized for vehicle-to-everything (V2X) communications. In [21], we analyzed the performance of multiple RIS-based vehicular communications over double Generalized-Gamma (dGG) fading model. In the aforementioned research, the direct signal received from the

This work was supported in part by the Science and Engineering Research Board (SERB), Department of Science and Technology (DST), Government of India, under MATRICS Grant MTR/2021/000890 and Start-up Research Grant SRG/2019/002345.

source is ignored. It should be noted that there can be a direct transmission link from the source to the destination in addition to the reflected signal through RIS elements, which has been studied in [7], [8] [17], [19]. However, the performance analysis is limited to asymptotic bounds and approximations considering simpler fading models. To the best of authors' knowledge an exact analysis for RIS-aided transmissions with direct link over double generalized (dGG) fading that accurately models the vehicular communications has not been reported in the literature [22]. It should be mentioned that deriving the statistics of the end-to-end SNR for the finite sum of the direct link and product of channel coefficients each distributed according to the dGG is quite involved.

In this paper, we analyze the performance of a RIS-assisted transmission scheme by coherently combining received signals reflected by RIS elements and direct transmissions from the source terminal for an enhanced connectivity in vehicular communications. We present analytical expressions on the outage probability and average BER performance by deriving exact density and distribution functions for the end-to-end SNR of the considered system. We also develop diversity order of the system by deriving asymptotic expressions on the outage probability and average BER for better Engineering insights on the system performance at high SNR. We demonstrate scaling of the system performance with RIS elements and a comparison to the conventional relaying techniques and direct transmissions considering various practically relevant scenarios.

Notations: $\Gamma(t) = \int_0^\infty s^{t-1} e^{-s} ds$ denotes the Gamma function, $\Gamma(a, t) = \int_t^\infty s^{a-1} e^{-s} ds$ denotes the incomplete Gamma function, $H_{p,q}^{m,n} \left(x \mid \begin{matrix} (a_1, A_1), \dots, (a_p, A_p) \\ (b_1, B_1), \dots, (b_q, B_q) \end{matrix} \right)$ denotes the Fox's H function, a notation for $\{a_i\}_1^N = \{a_1, \dots, a_N\}$, and j denotes the imaginary number.

II. SYSTEM MODEL

We consider a transmission model where a single-antenna source (S) communicates to a single-antenna destination (D) through an RIS with N reflecting elements, as shown in Fig. 1. We also consider direct transmission link which may be useful for an enhanced vehicular connectivity. We consider that the elements of RIS are spaced half of the wavelength and assume independent channels at the RIS [3], [10]. Assuming perfect knowledge of channel phase at each RIS element, the signal received at the destination is given as [7]:

$$y = \sqrt{P_t} s (h_{l_{ris}} \sum_{i=1}^N |h_{i,1}| |h_{i,2}| + h_l |h_d|) + v \quad (1)$$

where P_t is the transmit power, s is the unit power information bearing signal, $|h_{i,1}|$ and $|h_{i,2}|$ are channel fading coefficients between the source to the i -th RIS element and between the i -th RIS element to the destination, respectively, $|h_d|$ is the flat fading coefficient between source and destination, and v is the additive Gaussian noise with zero mean and variance σ_v^2 .

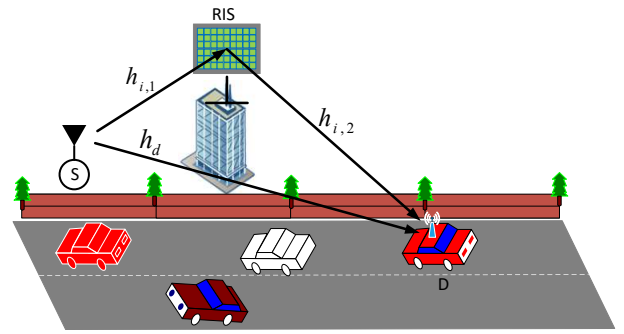


Fig. 1: System Model.

The path loss $h_{l_{ris}}$ of the cascaded link can be modeled using the free-space channel modeling of RIS-assisted communications [13], [23] as $h_{l_{ris}} = \frac{\sqrt{G_t G_r} c^2}{16\pi f^2 d_1 d_2}$, where G_t , G_r represent transmit and receive antenna gains, c is speed of the light, f is frequency of operation, d_1 and d_2 are the distances from source to RIS and RIS to destination respectively. The path loss component of direct transmission is given as $h_l = \frac{\sqrt{G_t G_r} c}{4\pi f \sqrt{d_1^2 + d_2^2}}$. We ignore the heights of source and destination to compute the path loss for direct link. We assume short-term fading coefficients $|h_{i,1}|$, $|h_{i,2}|$, and $|h_d|$ to be independent but non-identical distributed according to the dGG [22]. The Fox's H representation of the probability density function (PDF) for a dGG random variable $X(\alpha_1, \beta_1, \alpha_2, \beta_2)$ is given by [21]:

$$f_X(x) = \psi x^{\alpha_2 \beta_2 - 1} H_{0,2}^{2,0} \left[\phi x^{\alpha_2} \mid (0, 1), \left(\frac{\alpha_1 \beta_1 - \alpha_2 \beta_2}{\alpha_1}, \frac{\alpha_2}{\alpha_1} \right) \right] \quad (2)$$

where $\psi = \frac{\alpha_2}{\left(\frac{\Omega_1}{\beta_1}\right)^{\frac{\alpha_2 \beta_2}{\alpha_1}} \left(\frac{\Omega_2}{\beta_2}\right)^{\beta_2} \Gamma(\beta_1) \Gamma(\beta_2)}$, $\phi = \frac{\beta_2}{\Omega_2} \left(\frac{\beta_1}{\Omega_1}\right)^{\frac{\alpha_2}{\alpha_1}}$, α_1 , β_1 , α_2 , β_2 are Gamma distribution shaping parameters and $\Omega_i = \left(\frac{\mathbb{E}[X_i^2] \Gamma(\beta_i)}{\Gamma(\beta_i + 2/\alpha_i)}\right)^{\alpha_i/2}$, $i = 1, 2$ is the α_i -root mean value.

III. PERFORMANCE ANALYSIS

To facilitate performance analysis, the distribution function of $Z = h_{RIS} + h_d = \sum_{i=1}^N |h_{i,1}| |h_{i,2}| + |h_d|$ is required, where $|h_{i,1}| \sim dGG(\alpha_{i,1}, \beta_{i,1}, \alpha_{i,2}, \beta_{i,2})$, $|h_{i,2}| \sim dGG(\alpha_{i,3}, \beta_{i,3}, \alpha_{i,4}, \beta_{i,4})$ and $|h_d| \sim dGG(\alpha_{d,1}, \beta_{d,1}, \alpha_{d,2}, \beta_{d,2})$. We denote $\{a_i\}_1^N = \{a_1, \dots, a_N\}$ and imaginary number by j .

In what follows, we derive PDF and cumulative distribution function (CDF) of the sum of the product of dGG random variables (in Theorem 1) to develop statistical results of the end-to-end SNR of the considered system (in Theorem 2).

Theorem 1. *If $|h_{i,1}|$, $|h_{i,2}|$ are i.n.i.d random variables and distributed according to (2) and $h_i = |h_{i,1}| |h_{i,2}|$, then the*

PDF and CDF of $h_{\text{RIS}} = \sum_{i=1}^N h_i$ are given as

$$f_{h_{\text{RIS}}}(z) = z^{-1} \prod_{i=1}^N A_i B_i^{\beta_{i,2}} H_{0,1:1,4;\dots;1,4}^{0,0:4,1;\dots;4,1} \left[U(z) \left| \begin{array}{c} - : V_1 \\ (1; \{\alpha_{j,2}\}_{j=1}^N) : V_2 \end{array} \right. \right] \quad (3)$$

$$F_{h_{\text{RIS}}}(z) = \prod_{i=1}^N A_i B_i^{\beta_{i,2}} H_{0,1:1,4;\dots;1,4}^{0,0:4,1;\dots;4,1} \left[U(z) \left| \begin{array}{c} - : V_1 \\ (0; \{\alpha_{j,2}\}_{j=1}^N) : V_2 \end{array} \right. \right] \quad (4)$$

where $U(z) = \{\frac{z^{\alpha_{j,2}}}{B_j}\}_{j=1}^N$, $V_1 = \{(1, \alpha_{j,2})\}_{j=1}^N$, $V_2 = \{(\beta_{i,2}, 1), \{(\beta_{i,j}, \frac{\alpha_{i,2}}{\alpha_{i,j}})\}_{j=1,3,4}\}_{i=1}^N$, $A_i = \frac{\psi_{i,1} \psi_{i,2}}{\alpha_{i,4}} (\phi_{i,2})^{\frac{\alpha_{i,2} \beta_{i,2} - \alpha_{i,4} \beta_{i,4}}{\alpha_{i,4}}}$ and $B_i = \phi_{i,1}^{-1} (\phi_{i,2})^{-\frac{\alpha_{i,2}}{\alpha_{i,4}}}$.

Proof: See Appendix A. ■

Applying maximal ratio combining (MRC) at the destination for the received signals from RIS and direct transmissions, an expression for the resultant SNR is given as $\gamma = \gamma_{\text{RIS}} + \gamma_d = \gamma_{0,\text{RIS}} h_{\text{RIS}}^2 + \gamma_{0,d} |h_d|^2$, where $\gamma_{0,\text{RIS}} = \frac{h_{\text{ris}}^2 P_t}{\sigma_v^2}$ and $\gamma_{0,d} = \frac{h_d^2 P_t}{\sigma_v^2}$ represents average SNR for RIS and direct transmissions, respectively.

Theorem 2. The PDF and CDF of the resultant SNR $\gamma = \gamma_{\text{RIS}} + \gamma_d$ are given as

$$f_\gamma(\gamma) = \frac{1}{4} \psi_d \phi_d^{-\beta_{d,2}} \gamma^{-1} \prod_{i=1}^N A_i B_i^{\beta_{i,2}} H_{1,2:1,4;\dots;1,4;1,2}^{0,1:4,1;\dots;4,1;2,1} \left[U(\gamma) \left| \begin{array}{c} (1; \{\frac{\alpha_{j,2}}{2}\}_{j=1}^N, 0) : V_1 \\ (1; \{\frac{\alpha_{j,2}}{2}\}_{j=1}^N, \frac{\alpha_{d,2}}{2}), (1; \{\alpha_{j,2}\}_{j=1}^N, 0) : V_2 \end{array} \right. \right] \quad (5)$$

$$F_\gamma(\gamma) = \frac{1}{4} \psi_d \phi_d^{-\beta_{d,2}} \prod_{i=1}^N A_i B_i^{\beta_{i,2}} H_{1,2:1,4;\dots;1,4;1,2}^{0,1:4,1;\dots;4,1;2,1} \left[U(\gamma) \left| \begin{array}{c} (1; \{\frac{\alpha_{j,2}}{2}\}_{j=1}^N, 0) : V_1 \\ (0; \{\frac{\alpha_{j,2}}{2}\}_{j=1}^N, \frac{\alpha_{d,2}}{2}), (1; \{\alpha_{j,2}\}_{j=1}^N, 0) : V_2 \end{array} \right. \right] \quad (6)$$

where $U(\gamma) = \{\{\frac{1}{B_j} (\sqrt{\frac{\gamma}{\gamma_{0,\text{RIS}}}})^{\alpha_{j,2}}\}_{j=1}^N, (\phi_d (\sqrt{\frac{\gamma}{\gamma_{0,d}}})^{\alpha_{d,2}})\}$, $V_1 = \{\{(1, \alpha_{j,2})\}_{j=1}^N; (1, \frac{\alpha_{d,2}}{2})\}$, $V_2 = \{\{(\beta_{i,2}, 1), \{(\beta_{i,j}, \frac{\alpha_{i,2}}{\alpha_{i,j}})\}_{j=1,3,4}\}_{i=1}^N; (\beta_{d,2}, 1), (\beta_{d,1}, \frac{\alpha_{d,2}}{\alpha_{d,1}})\}$.

Proof: See Appendix B. ■

In what follows, we use the statistical results of Theorem 2 to analyze the system performance using outage probability and average BER.

A. Outage Probability

The outage probability P_{out} is defined as the probability of SNR failing to reach a threshold value, γ_{th} . An exact expression for the outage probability is given as $P_{\text{out}} = Pr(\gamma \leq \gamma_{\text{th}}) = F_\gamma(\gamma_{\text{th}})$. We use [24, eq. 30] to express outage probability asymptotically at high SNR as

$$P_{\text{out}}^\infty = \frac{1}{4} \psi_d \phi_d^{-\beta_{d,2}} \prod_{i=1}^N A_i B_i^{\beta_{i,2}} \prod_{i=1}^N (\frac{\gamma_{\text{th}}}{\gamma_0})^{p_i/2} \frac{\Gamma(\beta_{i,1} - \frac{p_i}{\alpha_{i,1}}) \Gamma(\beta_{i,2} - \frac{p_i}{\alpha_{i,2}}) \Gamma(\beta_{i,3} - \frac{p_i}{\alpha_{i,3}}) \Gamma(\beta_{i,4} - \frac{p_i}{\alpha_{i,4}})}{\Gamma(p_i \alpha_{i,2}) (\frac{\gamma_{\text{th}}}{\gamma_0})^{p_d/2} \Gamma(\beta_{d,1} - \frac{p_d}{\alpha_{d,1}}) \Gamma(\beta_{d,2} - \frac{p_d}{\alpha_{d,2}})} \frac{\Gamma(p_d \alpha_{d,2})}{\Gamma(1 + \sum_{i=1}^N p_i \alpha_{i,2} + p_d \alpha_{d,2})} \frac{\Gamma(\sum_{i=1}^N \frac{p_i \alpha_{i,2}}{2})}{\Gamma(\sum_{i=1}^N p_i \alpha_{i,2})} \quad (7)$$

where $p_i = \min\{\alpha_{i,1} \beta_{i,1}, \alpha_{i,2} \beta_{i,2}, \alpha_{i,3} \beta_{i,3}, \alpha_{i,4} \beta_{i,4}\}$ and $p_d = \min\{\alpha_{d,1} \beta_{d,1}, \alpha_{d,2} \beta_{d,2}\}$. The outage diversity $G_{d,\text{out}}$

is obtained by expressing $P_{\text{out}}^\infty \propto \gamma_0^{-G_{d,\text{out}}}$ to get $G_{d,\text{out}} = \sum_{i=1}^N \min\{\frac{\alpha_{i,1} \beta_{i,1}}{2}, \frac{\alpha_{i,2} \beta_{i,2}}{2}, \frac{\alpha_{i,3} \beta_{i,3}}{2}, \frac{\alpha_{i,4} \beta_{i,4}}{2}\} + \min\{\frac{\alpha_{d,1} \beta_{d,1}}{2}, \frac{\alpha_{d,2} \beta_{d,2}}{2}\}$. It is clear that the diversity order depends on RIS elements and channel fading parameters of reflected and direct transmission links.

B. Average BER

Using the CDF, the average BER for various modulation schemes (parameterized through a and b) is given as

$$\bar{P}_e = a \sqrt{\frac{b}{4\pi}} \int_0^\infty e^{-b\gamma} \gamma^{-\frac{1}{2}} F_\gamma(\gamma) d\gamma \quad (8)$$

We substitute $F_\gamma(\gamma)$ from (6) in (8), use the definition of multivariate Fox's H-function, and interchange the order of integration to get

$$\begin{aligned} \bar{P}_e &= (a \sqrt{\frac{b}{4\pi}})^{\frac{1}{4}} \psi_d \phi_d^{-\beta_{d,2}} \prod_{i=1}^N A_i B_i^{\beta_{i,2}} \frac{1}{2\pi j} \int_{L_i} B_i^{-s_i} \gamma_0^{-\sum_{j=1}^N \frac{\alpha_{j,2} s_j}{2}} \\ &\Gamma(\beta_{i,1} - \frac{\alpha_{i,2}}{\alpha_{i,1}} s_i) \Gamma(\beta_{i,3} - \frac{\alpha_{i,2}}{\alpha_{i,3}} s_i) \Gamma(\beta_{i,4} - \frac{\alpha_{i,2}}{\alpha_{i,4}} s_i) \Gamma(\beta_{i,2} - s_i) \\ &\Gamma(\alpha_{i,2} s_i) \frac{1}{2\pi j} \int_{L_d} \phi_d^{s_d} \gamma_{0,d}^{-\frac{\alpha_{d,2} s_d}{2}} \Gamma(\frac{\alpha_{d,2} s_d}{2}) \Gamma(\beta_{d,1} - \frac{\alpha_{d,2}}{\alpha_{d,1}} s_d) \\ &\frac{\Gamma(\beta_{d,2} - s_d) \Gamma(\alpha - \frac{1}{2} - \frac{\alpha_{d,2} s_d}{2})}{\Gamma(\frac{1}{2} + \alpha) \Gamma(2\alpha - 1 - \alpha_{d,2} s_d)} \left(\int_0^\infty e^{-b\gamma} \gamma^{\alpha-1} d\gamma \right) ds_i ds_d \end{aligned} \quad (9)$$

where $\alpha = \frac{1 + \alpha_{d,2} s_d + \sum_{i=1}^N \alpha_{i,2} s_i}{2}$. We solve the integral as $\int_0^\infty e^{-b\gamma} \gamma^{\alpha-1} d\gamma = (\frac{1}{b})^\alpha \Gamma(\alpha)$ and use the definition of N -multivariate Fox's H-function [25, A.1] to get eq. (10), as shown at the top of the next page, where $U(\gamma_{0,\text{RIS}}, \gamma_{0,d}) = \{\{B_j^{-1} (\gamma_{0,\text{RIS}} b)^{-\frac{\alpha_{j,2}}{2}}\}_{j=1}^N, \phi_d (\gamma_{0,d} b)^{-\frac{\alpha_{d,2}}{2}}\}$, $V_1 = \{(1, \alpha_{j,2})_{j=1}^N, (1, \alpha_{d,2})\}$, $V_2 = \{\{(\beta_{i,2}, 1), \{(\beta_{i,j}, \frac{\alpha_{i,2}}{\alpha_{i,j}})\}_{j=1,3,4}\}_{i=1}^N; (\beta_{d,2}, 1), (\beta_{d,1}, \frac{\alpha_{d,2}}{\alpha_{d,1}})\}$.

Similar to outage probability, we can use [24, eq. 31] to express average BER asymptotically at high SNR to derive the diversity of the system as $G_{d,\text{ber}} = \sum_{i=1}^N \min\{\frac{\alpha_{i,1} \beta_{i,1} - 1}{2}, \frac{\alpha_{i,2} \beta_{i,2} - 1}{2}, \frac{\alpha_{i,3} \beta_{i,3} - 1}{2}, \frac{\alpha_{i,4} \beta_{i,4} - 1}{2}\} + \min\{\frac{\alpha_{d,1} \beta_{d,1} - 1}{2}, \frac{\alpha_{d,2} \beta_{d,2} - 1}{2}\}$. Note that ergodic capacity of the proposed system can be similarly derived and has been left for longer version of the paper.

TABLE I: dGG fading parameters

Scenario	RIS: $\{(\alpha_1, \beta_1), (\alpha_2, \beta_2)\}$, DT: $\{(\alpha_{d,1}, \beta_{d,1}), (\alpha_{d,2}, \beta_{d,2})\}$
FP1	$\{(2,1), (2,2)\}, \{(1.5,1.5), (1,1.5)\}$
FP2	$\{(1,1), (1,2)\}, \{(2,1.5), (2,1.5)\}$
FP3	$\{(1,1.5), (1,2.5)\}, \{(2,2,1), (2,2,1)\}$

IV. SIMULATION AND NUMERICAL RESULTS

In this section, we validate the derived analytical expressions through Monte-Carlo simulations (averaged over 10^8 channel realizations) and numerical results. We consider carrier frequency $f = 6\text{GHz}$, antenna gains $G_T = 10\text{dBi}$, $G_R = 0\text{dBi}$, distance from source to RIS, $d_1 = 50\text{m}$ and

$$\bar{P}_e = \left(\alpha \sqrt{\frac{1}{4\pi}} \right)^{\frac{1}{4}} \psi_d \phi_d^{-\beta_{d,2}} \prod_{i=1}^N A_i B_i^{\beta_{i,2}} H_{2,2:1,4;\dots;1,4;1,2,1}^{0,2:4,1;\dots;4,1;2,1} \left[U(\gamma_{0,RIS}, \gamma_{0,d}) \left| \begin{array}{l} (\frac{1}{2}; \{\frac{\alpha_{j,2}}{2}\}_{j=1}^N, \frac{\alpha_{d,2}}{2}), (1; \{\frac{\alpha_{j,2}}{2}\}_{j=1}^N, 0) : V_1 \\ (0; \{\frac{\alpha_{j,2}}{2}\}_{j=1}^N, \frac{\alpha_{d,2}}{2}), (1; \{\alpha_{j,2}\}_{j=1}^N, 0) : V_2 \end{array} \right. \right] \quad (10)$$

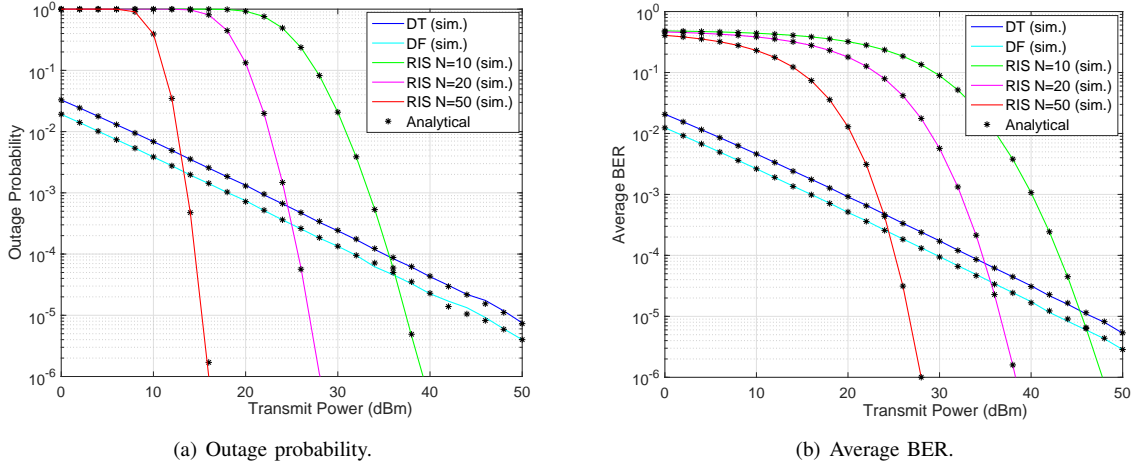


Fig. 2: Performance scaling of the RIS-assisted link compared with the DT and relaying systems.

RIS to destination, $d_2 = 100\text{m}$. A noise floor of -74dBm is considered over a 20MHz channel bandwidth. We assume identical dGG parameters for both the hops involving RIS and for each RIS element i.e., $\alpha_{i,1} = \alpha_{i,3} = \alpha_1$ and $\alpha_{i,2} = \alpha_{i,4} = \alpha_2 \forall i$. We use 3 different sets of dGG fading parameters (FP) summarized in table I with $\Omega_1 = 1.5793, \Omega_2 = 0.9671$. For numerical analysis, we used Python code implementation of multivariable Fox's H-function [26].

We demonstrate the performance scaling of RIS-assisted link (without considering signal from direct transmission (DT)) with number of RIS elements to achieve the performance of stable direct transmission (if available) and decode-and-forward (DF) relaying system for FP1 scenario, as shown in Fig. 2. The plots in Fig. 2(a) and Fig. 2(b) clearly indicate the number of RIS elements required to achieve DT and relaying performance for a given transmit power. Fig. 2(a) shows that the outage performance at a lower transmit power is not better due to the multiplicative effect of path loss and short-term fading of the RIS-assisted transmission when compared with DT and relaying systems. However, with an increase in transmit power, the RIS performance surpasses the DT and relaying system for a given N . The figure shows the direct link performance is better at low transmit powers, and the RIS-system enhances the reliability of the overall system at a higher transmit power. It can be seen that $N = 50$ RIS elements are required to achieve DT performance at $P_t = 15\text{dBm}$ and just $N = 20$ RIS elements at transmit power of 25dBm . Similarly, Fig. 2(b) shows the average BER performance of the RIS-system for a DPBSK modulation scheme with $a = 1$ and $b = 1$ such that the RIS performance becomes better than the DT and relaying for a given transmit power for a large RIS. Further, slope of the plots in Fig. 2(a) and Fig. 2(b) verify the

diversity order of the system.

Finally, we demonstrate the performance of RIS-assisted vehicular communications supplemented by the signal from direct transmissions, as depicted in Fig. 3. We consider a higher channel fading scenario (FP1) for the direct link and three different fading scenarios (FP1, FP2, and FP3) for the RIS-assisted link. It can be seen that the combined effect of RIS and direct transmission significantly improves the performance at a high transmit power and with a large RIS. As such, for $N = 10$ and transmit power less than 15 dBm , the performance is dictated by the direct link. However, there is a gain of 15 dBm to achieve an outage probability of 10^{-4} when N is increased from 10 to 50. Comparing FP2 and FP3 scenarios, the performance improves with the increase in shape parameter due to reduction in fading severity: a saving of 5dBm transmit power when β_1 is changed from 1 to 1.5 and β_2 from 2 to 2.5. Fig. 3(b) also demonstrates that the BER performance of the combined system is significantly better than the direct transmission at a high transmit power by harnessing the line-of-sight signal from the RIS elements. Moreover, the performance of RIS combined with direct transmission is always better than RIS alone (without DT) even at low SNR. Hence, it is clear that combined system performance is better than individual systems thereby exploiting the presence of DT at low SNRs and the signal received through RIS at high SNRs. It can be seen that the diversity order depends on fading parameters and RIS-elements N .

V. CONCLUSION

In this paper, we analyzed the performance of a RIS-assisted wireless system that coherently combines the received signals from direct transmission and reflected signals from the RIS

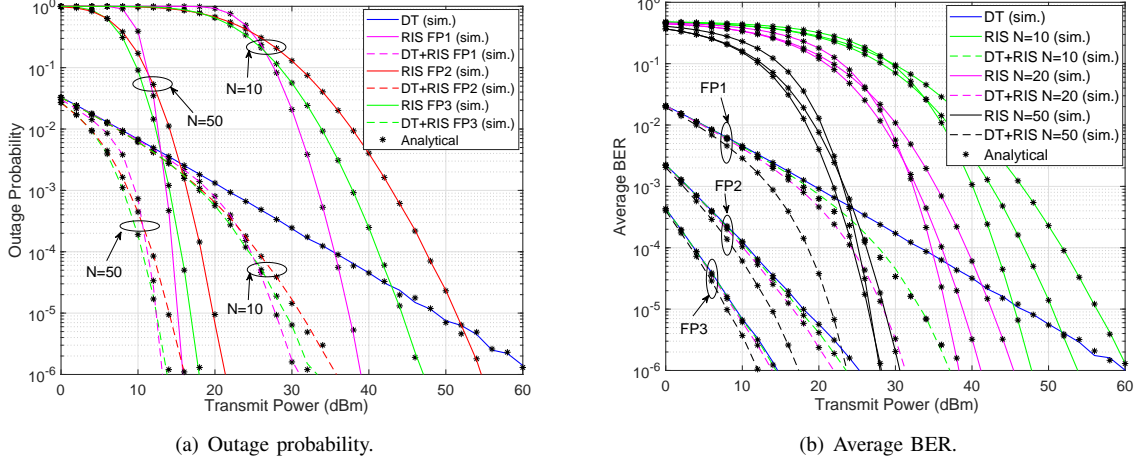


Fig. 3: Performance of RIS-assisted system with direct transmissions.

module. We derived exact closed-form expressions of PDF and CDF of the end-to-end SNR considering dGG fading channel models. We presented outage and average BER performance of the considered system in terms of multivariate Fox's H-function. We also derived simplified expressions at high SNR in terms of gamma functions to compute the diversity order of the system. We used computer simulations to deduce the scaling of RIS-assisted performance compared with the direct transmissions and the conventional relaying system. Further, harnessing the signal from direct link improves significantly the performance of RIS-assisted vehicular network. Our analysis demonstrates the effectiveness of the coherent combining of reflected signals from RIS and the signal from direct link to achieve reliable performance for a wide SNR range compared with individual systems.

It would be interesting to analyze the system performance considering a mobility model for the vehicular network. Further, the impact of correlated channels and imperfect phase compensation can be investigated as a future scope of the proposed work.

APPENDIX A: PDF AND CDF OF h_{RIS}

Using $f_{h_i}(z) = \int_0^\infty f_{|h_{i,1}|}(u)f_{|h_{i,2}|}\left(\frac{z}{u}\right)\frac{1}{u}du$ with identity [25], 2.3, we get the PDF of product of two random variables $h_i = |h_{i,1}||h_{i,2}|$ as

$$f_{h_i}(z) = A_i z^{\alpha_{i,2}\beta_{i,2}-1} H_{0,4}^{4,0} \left[B_i^{-1} z^{\alpha_{i,2}} \mid \begin{matrix} - \\ V_1 \end{matrix} \right] \quad (11)$$

Next, we use the definition of moment generating function (MGF) $M_{h_i}(s) = \int_0^\infty e^{-sz} f_{h_i}(z) dz$ and use the identity [25], 2.3 to get

$$M_{h_i}(s) = A_i s^{-\alpha_{i,2}\beta_{i,2}} H_{1,4}^{4,1} \left[B_i^{-1} s^{-\alpha_{i,2}} \mid \begin{matrix} (1 - \alpha_{i,2}\beta_{i,2}, \alpha_{i,2}) \\ V_1 \end{matrix} \right] \quad (12)$$

Using the product of MGF functions with the inverse Laplace transform, we get the PDF of $h_{\text{RIS}} = \sum_{i=1}^N h_i$ as $f_{h_{\text{RIS}}}(z) =$

$\mathcal{L}^{-1} \prod_{i=1}^N M_{h_i}(s)$. Thus, we use (12), expand the definition of Fox's H-function, and interchange the order of integration to get

$$f_{h_{\text{RIS}}}(z) = \prod_{i=1}^N A_i \frac{1}{2\pi j} \int_{L_i} B_i^{-s_i} \Gamma(\beta_{i,1} - \frac{\alpha_{i,2}}{\alpha_{i,1}} \beta_{i,2} - \frac{\alpha_{i,2}}{\alpha_{i,1}} s_i) \Gamma(-s_i) \Gamma(\beta_{i,4} - \frac{\alpha_{i,2}}{\alpha_{i,4}} \beta_{i,2} - \frac{\alpha_{i,2}}{\alpha_{i,4}} s_i) \Gamma(\beta_{i,3} - \frac{\alpha_{i,2}}{\alpha_{i,3}} \beta_{i,2} - \frac{\alpha_{i,2}}{\alpha_{i,3}} s_i) \Gamma(\alpha_{i,2}\beta_{i,2} + \alpha_{i,2}s_i) \left(\frac{1}{2\pi j} \int_{L'} s^{\sum_{i=1}^N -\alpha_{i,2}\beta_{i,2} - \alpha_{i,2}s_i} e^{sz} dt \right) ds_i \quad (13)$$

We apply [27, 8.315.1] to solve the inner integral in (13) as

$$\int_{L'} s^{\sum_{i=1}^N -\alpha_{i,2}\beta_{i,2} - \alpha_{i,2}s_i} e^{sz} ds = \frac{2\pi j z^{\sum_{i=1}^N \alpha_{i,2}\beta_{i,2} + \alpha_{i,2}s_i - 1}}{\Gamma(\sum_{i=1}^N \alpha_{i,2}\beta_{i,2} + \alpha_{i,2}s_i)} \quad (14)$$

We use (14) in (13) and apply the definition of N -multivariate Fox's H-function in [25, A.1] to get (3). We use similar steps to compute the CDF as $F_{h_{\text{RIS}}}(z) = \mathcal{L}^{-1} \frac{\prod_{i=1}^N M_{h_i}(s)}{s}$ to get (4).

APPENDIX B: PDF AND CDF OF $\gamma = \gamma_{\text{RIS}} + \gamma_d$

To derive the PDF of $\gamma = \gamma_{\text{RIS}} + \gamma_d$, we first compute the MGF of γ_{RIS} and γ_d and apply the inverse Laplace transform to find the PDF. For MGF of γ_{RIS} , we use its PDF and expand the definition of multivariate Fox's H-function and interchange the order of integration to get

$$M_{\gamma_{\text{RIS}}}(s) = \frac{1}{2} \prod_{i=1}^N A_i B_i^{\beta_{i,2}} \left(\frac{1}{2\pi j} \right)^N \int_{L_i} B_i^{-s_i} \gamma_{0,\text{RIS}}^{-\frac{\alpha_{i,2}s_i}{2}} \Gamma(\alpha_{i,2}s_i) \Gamma(\beta_{i,1} - \frac{\alpha_{i,2}}{\alpha_{i,1}} s_i) \Gamma(\beta_{i,3} - \frac{\alpha_{i,2}}{\alpha_{i,3}} s_i) \Gamma(\beta_{i,4} - \frac{\alpha_{i,2}}{\alpha_{i,4}} s_i) \frac{\Gamma(\beta_{i,2} - s_i)}{\Gamma(\sum_{j=1}^N \alpha_{j,2}s_j)} \left(\int_0^\infty \gamma^{\sum_{j=1}^N \frac{\alpha_{j,2}s_j}{2} - 1} e^{-s\gamma} d\gamma \right) ds_i \quad (15)$$

The inner integral is solved as $\int_0^\infty \gamma^{\sum_{j=1}^N \frac{\alpha_{j,2}s_j}{2} - 1} e^{-s\gamma} d\gamma = \left(\frac{1}{s} \right)^{\sum_{j=1}^N \frac{\alpha_{j,2}s_j}{2}} \Gamma(\sum_{j=1}^N \frac{\alpha_{j,2}s_j}{2})$.

Similarly, to get MGF of SNR of direct transmission, we express $e^{-s\gamma}$ in terms of Fox's H-function and use the identity [[25],2.3]

$$M_{\gamma_d}(s) = \frac{1}{2}\psi_d\phi_d^{-\beta_{d,2}}\frac{1}{2\pi j}\int_{L_d}\phi_d^{s_d}(s\gamma_{0,d})^{-\frac{s_d\alpha_{d,2}}{2}}\Gamma(\beta_{d,2}-s_d)\Gamma(\beta_{d,1}-\frac{\alpha_{d,2}}{\alpha_{d,1}}s_d)\Gamma(\frac{\alpha_{d,2}s_d}{2})ds_d \quad (16)$$

We solve the inner integral of PDF, $f_\gamma(\gamma) = \mathcal{L}^{-1}(M_{\gamma_{RIS}}(s)M_{\gamma_d}(s))$ as

$$\int_L (s)^{-\sum_{j=1}^N \frac{\alpha_{j,2}s_j}{2} - \frac{s_d\alpha_{d,2}}{2}} e^{s\gamma} ds = \frac{2\pi j\gamma^{\sum_{j=1}^N \frac{\alpha_{j,2}s_j}{2} + \frac{s_d\alpha_{d,2}}{2} - 1}}{\Gamma(\sum_{j=1}^N \frac{\alpha_{j,2}s_j}{2} + \frac{s_d\alpha_{d,2}}{2})} \quad (17)$$

Finally, we apply the definition of N -multivariate Fox's H-function in [25, A.1], to get (5). To compute the CDF of SNR, we use eq. (5) in $F_\gamma(\gamma) = \int_0^\gamma f_\gamma(x)dx$ and expand N -multivariate Fox's H-function in terms of Mellin-Barnes integrals to get

$$F_\gamma(\gamma) = \frac{1}{4}\psi_d\phi_d^{-\beta_{d,2}}\prod_{i=1}^N A_i B_i^{\beta_i,2} (\frac{1}{2\pi j})^N \int_{L_i} B_i^{-s_i} \gamma_{0,RIS}^{-\frac{\alpha_{i,2}s_i}{2}} \Gamma(\alpha_{i,2}s_i)\Gamma(\beta_{i,1}-\frac{\alpha_{i,2}}{\alpha_{i,1}}s_i)\Gamma(\beta_{i,3}-\frac{\alpha_{i,2}}{\alpha_{i,3}}s_i)\Gamma(\beta_{i,4}-\frac{\alpha_{i,2}}{\alpha_{i,4}}s_i) \Gamma(\beta_{i,2}-s_i)\frac{1}{2\pi j}\int_{L_d}\phi_d^{s_d}(s\gamma_{0,d})^{-\frac{s_d\alpha_{d,2}}{2}}\Gamma(\beta_{d,2}-s_d) \frac{\Gamma(\beta_{d,1}-\frac{\alpha_{d,2}}{\alpha_{d,1}}s_d)\Gamma(\frac{\alpha_{d,2}s_d}{2})\Gamma(\sum_{j=1}^N \frac{\alpha_{j,2}s_j}{2})}{\Gamma(\sum_{j=1}^N \frac{\alpha_{j,2}s_j}{2} + \frac{s_d\alpha_{d,2}}{2})\Gamma(\sum_{j=1}^N \alpha_{j,2}s_j)} (\int_0^\infty x^{\sum_{j=1}^N \frac{\alpha_{j,2}s_j}{2} + \frac{s_d\alpha_{d,2}}{2} - 1} dx) ds_i ds_d \quad (18)$$

Now, the inner integral can be solved as

$$I = \frac{\Gamma(\sum_{j=1}^N \frac{\alpha_{j,2}s_j}{2} + \frac{s_d\alpha_{d,2}}{2})\gamma^{\sum_{j=1}^N \frac{\alpha_{j,2}s_j}{2} + \frac{s_d\alpha_{d,2}}{2}}}{\Gamma(\sum_{j=1}^N \frac{\alpha_{j,2}s_j}{2} + \frac{s_d\alpha_{d,2}}{2} + 1)} \quad (19)$$

We substitute (19) in (18) and apply the definition of N -multivariate Fox's H-function to get (6).

REFERENCES

- [1] Y. Zhu, B. Mao, Y. Kawamoto, and N. Kato, "Intelligent reflecting surface-aided vehicular networks toward 6G: Vision, proposal, and future directions," *IEEE Veh. Technol. Mag.*, vol. 16, no. 4, pp. 2–10, Dec. 2021.
- [2] Q. Wu, S. Zhang, B. Zheng, C. You, and R. Zhang, "Intelligent reflecting surface aided wireless communications: A tutorial," *IEEE Trans. Commun.*, vol. 69, no. 5, pp. 3313–3351, Jan. 2021.
- [3] E. Basar, M. D. Renzo, J. D. Rosny, M. Debbah, M. S. Alouini, and R. Zhang, "Wireless communications through reconfigurable intelligent surfaces," *IEEE Access*, vol. 7, pp. 116753–116773, Aug. 2019.
- [4] D. Kudathanthirige, D. Gunasinghe, and G. Amarasureya, "Performance analysis of intelligent reflective surfaces for wireless communication," in *ICC 2020-2020 IEEE Int. Conf. Commun. (ICC)*, Dublin, Ireland, July 2020, pp. 1–6.
- [5] Q. Tao, J. Wang, and C. Zhong, "Performance analysis of intelligent reflecting surface aided communication systems," *IEEE Commun. Lett.*, vol. 24, no. 11, pp. 2464–2468, July 2020.
- [6] R. C. Ferreira, M. S. P. Facina, F. A. P. De Figueiredo, G. Fraidenraich, and E. R. De Lima, "Bit error probability for large intelligent surfaces under double-Nakagami fading channels," *IEEE Open J. Commun. Society*, vol. 1, pp. 750–759, May 2020.
- [7] D. Selimis, K. P. Peppas, G. C. Alexandropoulos, and F. I. Lazarakis, "On the performance analysis of RIS-empowered communications over Nakagami-m fading," *IEEE Commun. Lett.*, vol. 25, no. 7, pp. 2191–2195, April 2021.
- [8] M. H. Khoshafa, T. M. N. Ngatched, M. H. Ahmed, and A. R. Ndjiongue, "Active reconfigurable intelligent surfaces-aided wireless communication system," *IEEE Commun. Lett.*, vol. 25, no. 11, pp. 3699–3703, Nov. 2021.
- [9] I. Trigui, W. Ajib, and W.-P. Zhu, "A comprehensive study of reconfigurable intelligent surfaces in generalized fading," [Online], arXiv: 2004.02922, 2020.
- [10] H. Du, J. Zhang, J. Cheng, Z. Lu, and B. Ai, "Millimeter wave communications with reconfigurable intelligent surfaces: Performance analysis and optimization," *IEEE Trans. Commun.*, vol. 69, no. 4, pp. 2752–2768, Jan. 2021.
- [11] V. Jamali, H. Ajam, M. Najafi, B. Schmauss, R. Schober, and H. V. Poor, "Intelligent reflecting surface assisted free-space optical communications," *IEEE Commun. Magazine*, vol. 59, no. 10, pp. 57–63, Nov. 2021.
- [12] V. K. Chapala and S. M. Zafaruddin, "Unified performance analysis of reconfigurable intelligent surface empowered free space optical communications," Accepted for publication in *IEEE Trans. Commun.*, Dec. 2021, arXiv: 2106.02000, 2021.
- [13] H. Du, J. Zhang, K. Guan, B. Ai, and T. Kürner, "Reconfigurable intelligent surface aided TeraHertz communications under misalignment and hardware impairments," [Online] arXiv: 2012.00267, 2020.
- [14] V. K. Chapala and S. M. Zafaruddin, "Exact Analysis of RIS-Aided THz Wireless Systems Over α - μ Fading with Pointing Errors," *IEEE Commun. Lett.*, vol. 25, no. 11, pp. 3508–3512, Nov. 2021.
- [15] J. Wang, W. Zhang, X. Bao, T. Song, and C. Pan, "Outage analysis for intelligent reflecting surface assisted vehicular communication networks," [Online], arXiv: 2004.08063, 2020.
- [16] K. Odeyemi, P. A. Owolawi, and O. O. Olakanmi, "Reconfigurable intelligent surface assisted mobile network with randomly moving user over Fisher-Snedecor fading channel," *Physical Communication*, vol. 43, p. 101186, Aug. 2020.
- [17] D. Dampahalage *et al.*, "Intelligent reflecting surface aided vehicular communications," [Online], arXiv: 2011.03071, 2020.
- [18] L. Kong, J. He, Y. Ai, S. Chatzinotas, and B. Ottersten, "Channel modeling and analysis of reconfigurable intelligent surfaces assisted vehicular networks," in *2021 IEEE Int. Conf. Commun. Workshops (ICC Workshops)*, Montreal, QC, Canada, June 2021, pp. 1–6.
- [19] Y. U. Ozcan, O. Ozdemir, and G. K. Kurt, "Reconfigurable intelligent surfaces for the connectivity of autonomous vehicles," *IEEE Trans. Vehi. Technol.*, vol. 70, no. 3, pp. 2508–2513, March 2021.
- [20] A. U. Makarfi, K. M. Rabie, O. Kaiwartya, X. Li, and R. Kharel, "Physical layer security in vehicular networks with reconfigurable intelligent surfaces," in *2020 IEEE 91st Veh. Tech. Conf. (VTC2020-Spring)*, May 2020, pp. 1–6.
- [21] V. K. Chapala and S. M. Zafaruddin, "RIS-assisted multihop FSO/RF hybrid system for vehicular communications over generalized fading," [Online], arXiv: 2112.12944, 2021.
- [22] P. S. Bithas, A. G. Kanatas, D. B. da Costa, P. K. Upadhyay, and U. S. Dias, "On the double-generalized gamma statistics and their application to the performance analysis of V2V communications," *IEEE Trans. Commun.*, vol. 66, no. 1, pp. 448–460, Jan. 2018.
- [23] W. Tang, M. Z. Chen, X. Chen *et al.*, "Wireless communications with reconfigurable intelligent surface: Path loss modeling and experimental measurement," *IEEE Trans. Wireless Commun.*, vol. 20, no. 1, pp. 421–439, Jan 2021.
- [24] Y. Abo Rahama, M. H. Ismail, and M. S. Hassan, "On the sum of independent Fox's H-function variates with applications," *IEEE Trans. Vehi. Technol.*, vol. 67, no. 8, pp. 6752–6760, 2018.
- [25] A. Mathai, R. K. Saxena, and H. J. Haubold, *The H-Function: Theory and Applications*. Springer New York, 2009.
- [26] H. R. Alhennawi *et al.*, "Closed-form exact and asymptotic expressions for the symbol error rate and capacity of the H-function fading channel," *IEEE Trans. Veh. Technol.*, vol. 65, no. 4, pp. 1957–1974, 2016.
- [27] I. Gradshteyn and I. M. Ryzhik, *Table of Integrals, Series, And Products*, Jan. 2007.